DOI: 10.1002/cmdc.200700170

# CMP-Pseudaminic Acid is a Natural Potent Inhibitor of PseB, the First Enzyme of the Pseudaminic Acid Pathway in *Campylobacter jejuni* and *Helicobacter pylori*

David J. McNally,* Ian C. Schoenhofen, R. Scott Houliston, Nam H. Khieu, Dennis M. Whitfield, Susan M. Logan, Harold C. Jarrell, and Jean-Robert Brisson[a]

*Campylobacter jejuni* is the leading cause of bacterial gastroenteritis worldwide and a significant cause of child morbidity in underdeveloped countries. There is also evidence linking *C. jejuni* infections to the development of Miller Fisher and Guillain-Barré neuropathies, the latter being the primary cause of neuroparalysis since the eradication of polio.[1] Approximately two-thirds of the world's population is infected with *Helicobacter pylori*,[2] which is a major etiological agent of gastroduodenal disease and the only bacterium associated with cancer.[3] As a result of the prevalence of infections caused by these pathogens and the increase in antibiotic resistant strains, novel therapeutics are urgently needed.

Glycan biosynthetic pathways in bacteria are attractive therapeutic targets as many of these glycans are associated with cell-surface virulence factors and are unique to prokaryotes. *C. jejuni* and *H. pylori* decorate their flagella extensively with the sialic acid-like sugar 5,7-diacetamido-3,5,7,9-tetradeoxy-L-*glycero*-α-L-*manno*-nonulosonic acid or pseudaminic acid (Pse).[4–6] Recently, *C. jejuni* was shown to decorate its flagellin with a number of structurally related nonulosonate derivatives as well.[7] *O*-linked flagellin glycosylation with Pse is necessary for proper assembly of flagellar filaments, bacterial motility, colonization, and hence virulence. Agents that interfere with Pse production may therefore offer therapeutic potential. Recently, we identified six Pse biosynthesis enzymes (PseB, C, H, G, I, F, Figure 1) which constitute the complete CMP-Pse biosynthetic pathway starting from UDP-α-D-GlcNAc (**1**).[6,8] The initial enzyme, PseB, is considered unique as it is a 4,6-dehydratase/5-epimerase that converts **1** to UDP-2-acetamido-2,6-dideoxy-β-L-*arabino*-hexos-4-ulose (**2**). By using $^1$H NMR as a real-time analytical probe to continuously follow the PseB reaction, it can be shown that upon accumulation of **2**, PseB catalyzes an additional C5 epimerization forming UDP-2-acetamido-2,6-dideoxy-α-D-*xylo*-hexos-4-ulose (**3**) (Supporting Information Figure S1).[6,9] In *C. jejuni*, **3** is used to make 2,4-diacetamido-2,4,6-

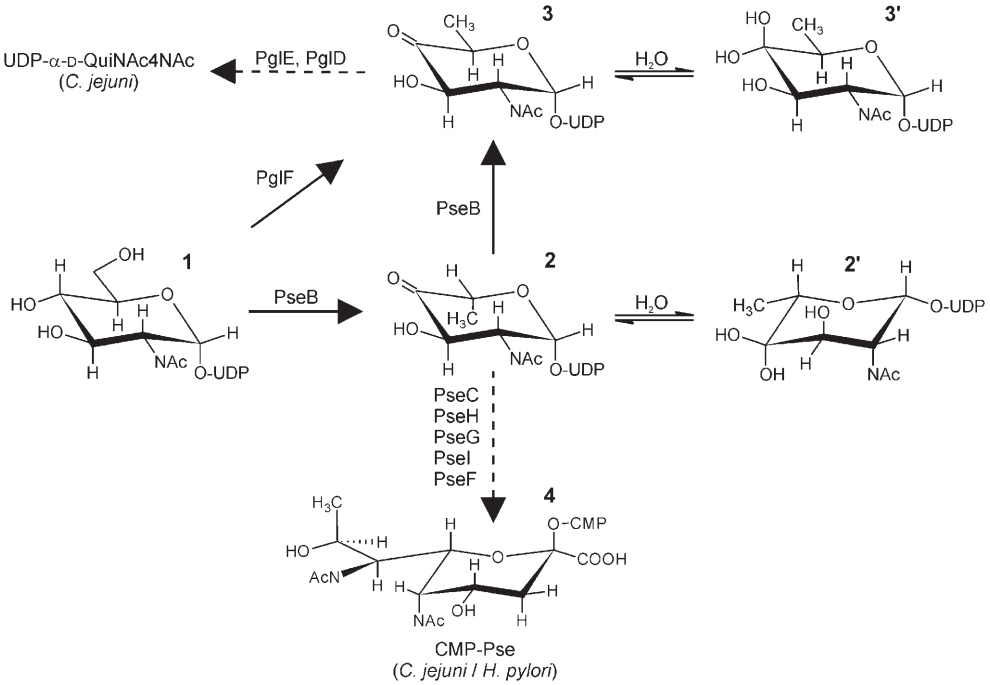


**Figure 1.** PseB catalyzed reactions with respect to the CMP-Pse and UDP-α-D-QuiNAc4NAc biosynthetic pathways.[6,8] **1**, UDP-α-D-GlcNAc; **2**, UDP-2-acetamido-2,6-dideoxy-β-L-*arabino*-hexos-4-ulose; **2**′, gem-diol form of **2**; **3**, UDP-2-acetamido-2,6-dideoxy-α-D-*xylo*-hexos-4-ulose; **3**′, gem-diol form of **3**, **4**, CMP-pseudaminic acid.

[a] *Dr. D. J. McNally, Dr. I. C. Schoenhofen, Dr. R. S. Houliston, N. H. Khieu, Dr. D. M. Whitfield, Dr. S. M. Logan, Dr. H. C. Jarrell, Dr. J.-R. Brisson*
*National Research Council of Canada-Institute for Biological Sciences, Ottawa ON, K1A 0R6 (Canada)*
*Fax: (+1) 613-952-9092*
*E-mail: david.mcnally@nrc-cnrc.gc.ca*

Supporting information for this article is available on the WWW under http://www.chemmedchem.org or from the author.

  

trideoxy-α-D-Glc (α-D-QuiNAc4NAc) which is an important component of the *N*-linked glycan that modifies over 30 proteins in this bacterium.[10] A control experiment confirmed that PseB is responsible for this additional C5 epimerization as **3** was never observed to be produced from **2** in solution when PseB was absent (not shown). This finding supports a metabolomics study that observed the accumulation of UDP-α-D-QuiNAc4NAc within a *pseC* mutant that suggested cross-talk between the Pse and α-D-QuiNAc4NAc pathways via PseB.[5] The dependence of *O*-linked flagellin glycosylation on PseB, and its possible contributions to other carbohydrate biosynthetic pathways make PseB a prime therapeutic target. Inhibition of PseB with a small molecule therefore presents an opportunity to pharmaceutically control infections caused by *C. jejuni* and *H. pylori*.

Mapping the dynamic interactions of a targeted protein with its ligand and potential inhibitors can facilitate the development of new inhibitors. Saturation transfer difference (STD) NMR is now widely used for studies examining the binding of carbohydrates to proteins.[11–13] STD NMR relies on the principle that when signals from a protein are selectively irradiated, ligands in exchange between the bound and the free forms will also become saturated. Subtraction of spectra acquired without protein irradiation reveals binding epitopes.[14] STD NMR is rapid, easy to implement, does not require isotope labeling of the protein or excessive quantities of protein, and qualitative interpretation of the spectra is straightforward.[11,14,15]

As an initial step towards the development of a small molecular inhibitor, binding epitopes were determined for PseB by monitoring the reaction directly in an NMR tube (13 °C) with proton and STD experiments at regular intervals (Figure 2). For **1**, the largest saturation transfer occurred at H1 of ribose indicating its close proximity to the protein. Substantial STD effects were also observed for ribose H4 and H5/5′, and for uracil H5 and H6. GlcNAc sugar ring resonances exhibited the lowest saturation transfer suggesting that it is farthest from the protein. As the UDP-hexos-4-ulose sugars **2** and **3** rapidly convert to their *gem*-diol forms in solution,[9] STD signals were only observed for **2**′ and **3**′. As is the case for **1**, the largest amount of saturation transfer for **2**′ and **3**′ occurred at ribose H1 followed by uracil resonances, whereas the sugar ring signals showed the lowest STD effect (Supporting Information Figures S2 and S3). Interestingly, we observed deuterium labeling at the H5 position of **2**′, as indicated by the singlet signal for H6, and no deuterium labeling at H6 (Supporting Information Figure S2). This finding conflicts with the reaction mechanism reported for PseB where it would be expected to see deuterium labeling at H6 but not at H5 as NADPH was proposed to protonate the 5 position.[16] Our NMR findings indicate that the PseB reaction mechanism more closely resembles that described for RmlB, which is a 4,6-dehydratase from the L-rhamnose pathway in *Salmonella enterica*.[17] Resonances originating from the 2-acetamido-2,6-dideoxy-α-D-*xylo*-hexos-4-ulose sugar ring of **3**′ showed the smallest STD effect compared to those for **1** and **2**′ indicating a minimal amount of interaction with PseB. This finding is consistent with **3** being an end product of the PseB reaction that accumulates with no further conversion to another product (Supporting Information Figure S1). Based on these STD NMR results, it was concluded that the nucleotide group in **1**, **2**′, and **3**′ is the key binding epitope for PseB. STD NMR experiments aimed at examining the interaction between PseB and UDP or GlcNAc-1-phosphate substantiated this hypothesis as UDP interacted strongly with the enzyme whereas GlcNAc-1-phosphate did not (Supporting Information Figures S4 and S5).

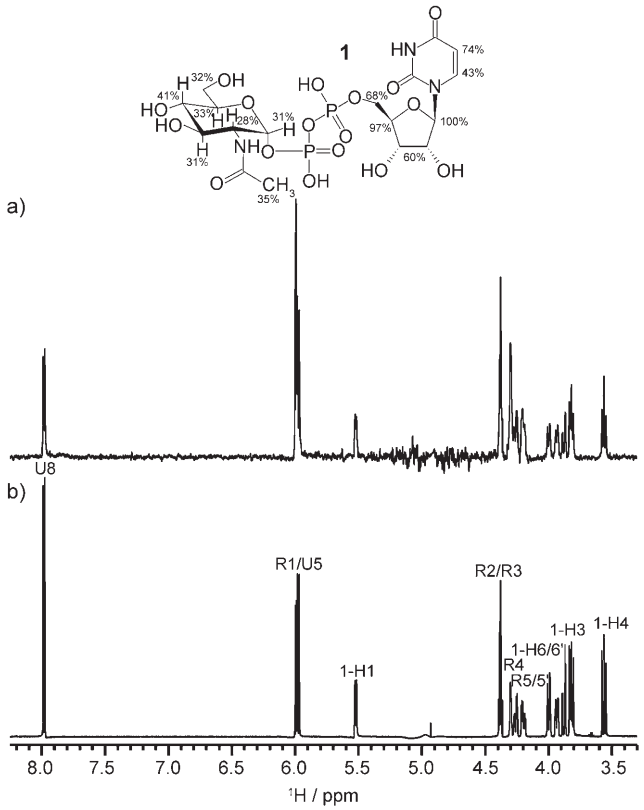


**Figure 2.** Examination of the PseB reaction (13 °C, Time 0 h) with STD NMR (600 MHz, $^1$H) showing binding epitopes for UDP-α-D-GlcNAc (**1**) (8% $H_2O$/92% $D_2O$, 25 mM $NaPO_4$, 25 mM NaCl, pH 7.3, 9.2 mM **1**, 530 μg or 46 μM PseB, substrate:protein 200:1). a) STD NMR spectrum (2 s saturation, 512 scans). b) Proton reference spectrum (16 scans). U represents uracil and R is ribose. STD effects for R2/3 and R5/5′ were calculated together because of overlap of these resonances.

During the recent characterization of the CMP-Pse biosynthetic pathway, we observed a sharp decrease in PseB activity following the accumulation of CMP-Pse that suggested it was a natural inhibitor.[8] Furthermore, UDP-α-D-Gal and UDP were reported to completely inhibit the PseB reaction.[18] To investigate these putative inhibitors, they were first assayed in a dose dependent manner with PseB (Supporting Information Figure S6). Our findings do not support the literature as UDP-α-D-Gal did not inhibit PseB, even when assayed at five times higher concentration than **1**. UDP only moderately inhibited PseB. In contrast, CMP-Pse is a potent inhibitor that completely inhibited the PseB reaction at very low concentrations (100 μM). From the double reciprocal plot shown in Figure 3, **4** was concluded to be a competitive inhibitor ($K_i$(app) = 18.7 μM) that competes directly with **1** for the active site of PseB.

  

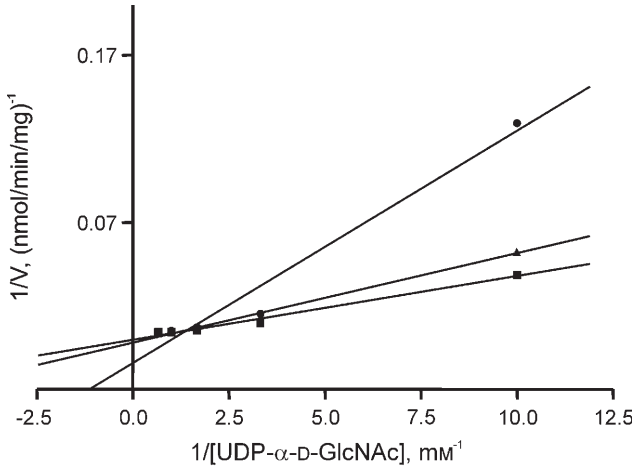


**Figure 3.** Double reciprocal plot for initial PseB reaction rates versus UDP-α-D-GlcNAc concentration in the presence of 0 μM (square), 5 μM (triangle), or 10 μM (circle) CMP-Pse. As can be seen from this kinetic analysis, CMP-Pse is a competitive inhibitor of PseB.

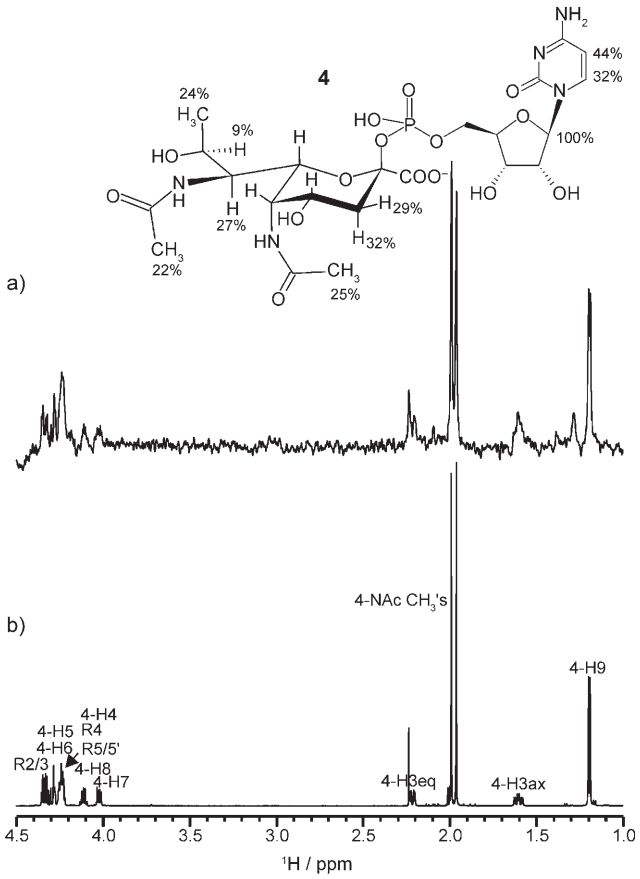


**Figure 4.** Mapping binding epitopes for CMP-Pse (**4**) with PseB using STD NMR (600 MHz, $^1$H) (25 °C, 3% $H_2O$/97% $D_2O$, 25 mM $NaPO_4$, 25 mM NaCl, pH 7.3, 4.4 mM **4**, 22.3 μM PseB, substrate:protein 200:1). a) STD NMR spectrum (2 s saturation, 3000 scans). b) Proton reference spectrum (128 scans). STD effects were not determined for R-2, R-3, R-4, R-5/5′ or for **4**-H4, **4**-H5, and **4**-H6 because of spectral overlap that prevented accurate integration measurements.

To characterize PseB inhibition by **4** at the molecular level, STD NMR was used to determine binding epitopes (Figure 4). Similar to **1**, **2**′, and **3**′, the largest saturation transfer for **4** occurred at H1 of ribose. H5 and H6 of cytosine also experienced large STD effects whereas the sugar ring and exocyclic chain (H7, H8, and H9) resonances received the lowest amount of transfer. Interestingly, STD signals for **4** were less intense compared to those for **1**, **2**′, or **3**′. This observation is consistent with **4** being an efficient inhibitor of PseB as high affinity ligands undergo slower chemical exchange (lower $k_{off}$) leading to diminished STD signals.[19] Attempts to determine the bioactive conformation of **4** bound to PseB using transferred NOESY (tr-NOESY) experiments were not successful, even at lower ligand-to-protein ratios (10:1, 2:1) as only positive NOEs originating from free **4** were observed (not shown). This finding was not unexpected as tr-NOEs are usually only observed for systems where exchange between the free and bound states of the ligand is fast on the NMR relaxation time scale.[12,15] As a control, identical STD and tr-NOESY conditions were used to determine binding epitopes and tr-NOEs for UDP-α-D-Gal (Supporting Information Figures S7 and S8). The UDP-α-D-Gal/PseB system is a suitable model as UDP-α-D-Gal was shown to interact with the active site of PseB.[16] According to our findings however, UDP-α-D-Gal does not inhibit PseB and therefore the rate of exchange would be faster compared to **4**.

Based on the crystal structure reported for PseB,[16] complete relaxation and conformational exchange matrix (CORCEMA) calculations and molecular modeling were used to validate the STD NMR findings and to study **4** docked within the active site of PseB. CORCEMA can be used to calculate STD NMR intensities for a ligand–protein complex if parameters such as correlation times, saturated protein protons, exchange rates, and spectrometer frequency are known.[20] Based on CORCEMA calculations, the largest transfer of saturation in **4** was predicted to occur at H1 of ribose (100%) and H6 of cytosine (91%), whereas the smallest was predicted to occur at H3eq (26%) and H9 (25%) of pseudaminic acid (Supporting Information Table S1). Discrepancies for observed and calculated STD intensities are likely attributable to factors that are not taken into account by the calculations such as internal motions of **4** and anisotropic movement of the PseB/CMP-Pse hexameric complex in solution. Superimposing the energy minimized models for **1** (red) and **4** (blue) docked within the PseB active site revealed conformational similarities for both ligands (Figure 5, Supporting Information Figures S9 and S10). **1** and **4** were found to have the same orientation and length within the PseB active site. Furthermore, the location and conformation of the pyrimidine rings and ribose sugars were nearly identical for both ligands. Interestingly, the **1**- and **4**-α-phosphates, and the **1**-β-phosphate and **4**-carboxylic acid group were found to occupy similar space in close proximity to arginine 199 and arginine 252. One may infer that electrostatic interactions with these negatively charged groups (yellow) stabilize **1** and **4** within the active site. Hydrophobic interactions may also stabilize **4** within the active site as the acetamido methyl protons located at the 5 and 7 positions of **4** were found to be proximal to the aromatic rings of tyrosine 135 and tryptophan 201,

  

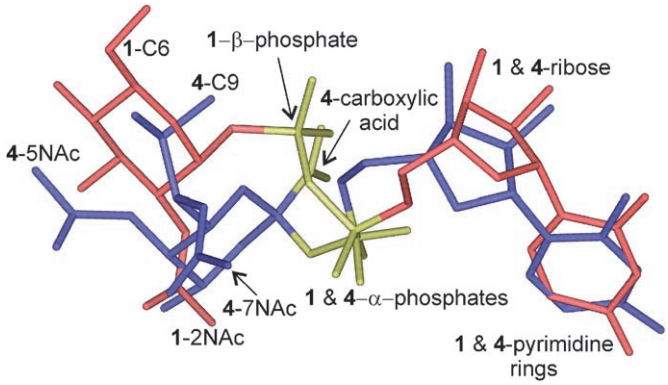


**Figure 5.** Energy minimized models for UDP-α-D-GlcNAc (**1**, red) and CMP-Pse (**4**, blue) docked within the PseB active site. As can be seen, the pyrimidine rings, ribose sugars, and negatively charged groups (yellow) of **1** and **4** occupy similar space. Models were constructed using the Autodock 3.0 software and the coordinates deposited for the crystal structure of PseB.[16]

respectively. CORCEMA calculations and molecular modeling therefore validated STD NMR findings and supported the nucleotide group as the key binding epitope.

Rational design strategies for a small molecule inhibitor may consider incorporating a nucleotide group or mimic as our findings show that it is the dominant binding epitope for PseB. There is more opportunity for experimentation/optimization with the carbohydrate moiety as PseB interacts with structurally diverse nucleotide-activated hexoses (**1**, **2**, UDP-α-D-Gal) and a nonulosonate (**4**). Nonulosonates may offer optimized levels of inhibition as the acetamido group located on the exocyclic chain establishes additional contacts with active site residues. Based on the fact that PseB is strongly inhibited by CMP-Pse, it can be concluded that Pse levels are feedback regulated within the bacterial cell and that PseB is a key control point for Pse production which underscores the importance of this enzyme as a therapeutic target. Regulation of CMP-Pse biosynthesis in *C. jejuni* and *H. pylori* more closely resembles CMP-sialic acid production (CMP-*N*-acetyl-neuraminic acid, CMP-NANA) in eukaryotes, which is also feedback regulated,[21] compared to CMP-NANA production in *E. coli* which is controlled by an aldolase.[22] Based on these findings and studies that have uncovered feedback inhibited carbohydrate pathways in other bacteria,[21,23] the sugar metabolome may be a valuable source of lead compounds and useful information for the development of small molecule inhibitors as antimicrobial therapies.

## Experimental Section

Recombinant *H. pylori* PseB was expressed and purified as previously reported.[6] STD NMR spectra were acquired at 13 °C or 25 °C on a Varian (Palo Alto, U.S.A.) spectrometer at 600 MHz ($^1$H) with a cryogenically cooled probe. STD experiments were carried out using an excess of ligand:protein (200:1) in buffered $D_2O$ (8% $H_2O$/92% $D_2O$, 25 mM $NaPO_4$, 25 mM NaCl, pH 7.3). Saturation of PseB resonances was achieved using a train of Gaussian-shaped pulses, with bandwidths of 300 Hz centred at −1.0 ppm. Phase cycling was used to subtract reference spectra (pulses centered at 30 ppm) from those where PseB resonances were excited. STD spectra were acquired using 2 s saturation time, a relaxation delay of 2.5 s, an acquisition time of 1.9 s, and the number of transients varied from 1024 to 3072. A spin-lock filter of 10 ms was used to suppress the protein background. STD effects are reported as a percentage of the resonance that received the largest absolute amount of saturation transfer, which was normalized to 100%. Absolute amounts of saturation transfer were determined for each resonance by comparing the ratio of signal-to-noise (S/N) in the STD spectrum to that in the proton spectrum. STD effects are reported only for resonances where accurate integration measurements could be obtained. Proton and STD spectra were referenced to an internal acetone standard ($\delta_H = 2.225$ ppm). For enzyme kinetic analysis, 10 μg of PseB was incubated at 37 °C in 200 μL of 25 mM $NaPO_4$ buffer (pH 7.3, 25 mM NaCl) containing various quantities of UDP-α-D-GlcNAc and CMP-Pse. An apparent $K_i$ value was derived using 0.6 mM UDP-α-D-GlcNAc measurements. Enzymatic reactions were analyzed by capillary electrophoresis according to Schoenhofen et al.[6] Substrate concentrations and conversions were determined using the molar extinction coefficients for UDP ($\varepsilon_{260} = 10\,000$) and CMP ($\varepsilon_{260} = 7400$). Kinetic plots were performed using the GraphPad Prism 3 software (GraphPad Software Inc., San Diego, U.S.A.). The Autodock 3.0 software was used to dock ligands into the PseB monomer.[24] Coordinates for PseB were extracted from the X-ray structure reported for the PseB dimer.[16] Grid maps were calculated at the PseB active site and a Lamarckian genetic algorithm was used to perform 100 docking experiments with a maximum number of $1.5 \times 10^6$ energy evaluations. Step sizes used were 0.2 Å for ligand translations, and 5° for ligand orientations and tortions. Figure 5 shows the lowest energy conformation for CMP-Pse docked within the PseB active site. Figures for molecular models were generated using the Insight II software (Accelrys, San Diego, U.S.A.). Details for CORCEMA-ST theory and calculations are described elsewhere.[20] For CORCEMA calculations, the generalized order parameter $S^2$ for intramethyl group relaxation was set to 0.25 whereas an $S^2$ of 0.85 was used for methyl-X relaxation; the ligand concentration was 8 mM; the ligand-to-protein ratio was 200:1; $K_{on}$ was $10^8$; $K_{eq}$ was varied from $10^3$ to $10^6$ with $2 \times 10^6$ giving the best fit compared to the experimental results (saturation time 2 s). The correlation time of the free ligand was set to 0.3 ns, whereas a correlation time of 80 ns was used for the PseB/CMP-Pse complex (hexameric form). Calculated STD signal intensities were evaluated as $100 \times [(I(0)_j - I(t)_j)/I(0)_j]$ with $I(t)_j$ and $I(0)_j$ corresponding to the intensity of proton j with and without saturation transfer during a saturation time *t*. Calculated relative saturation transfer intensities are expressed as the ratio of the STD intensity of proton *k* in the ligand to that of the ligand ribosyl H1.

## Acknowledgements

*The authors thank Denis Brochu and Tania Audy for technical assistance, Dr. N. R. Krishna (University of Alabama at Birmingham) for generously providing the CORCEMA-ST program, and Dr. H. Jennings (National Research Council of Canada) for financial support provided to D. J. McNally.*

**Keywords:** *Campylobacter jejuni* · Helicobacter *pylori* · inhibitors · pseudaminic acid · STD NMR spectroscopy

  

[1] a) B. C. Jacobs, P. H. Rothbarth, F. G. A. van Der Meché, P. Herbrink, P. I. M. Schmitz, M. A. de Klerk, P. A. van Doorn, *Neurology* **1998**, *51*, 1110 – 1115; b) J. Kelly, J. R. Brisson, N. M. Young, H. C. Jarrell, C. M. Szymanski, *Bacterial genomes and infectious diseases* (Eds.: V. L. Chan, P. M. Sherman, W. Burke), Humana, New Jersey, **2005**, pp. 63 – 90.
[2] D. Y. Graham, P. D. Klein, A. R. Opekun, T. W. Boutton, *J. Infect. Dis.* **1988**, *157*, 777 – 780.
[3] a) M. J. Blaser, *Gastroenterology* **1992**, *102*, 720 – 727; b) B. E. Dunn, H. Cohen, M. J. Blaser, *Clin. Microbiol. Rev.* **1997**, *10*, 720 – 741.
[4] P. Thibault, S. M. Logan, J. F. Kelly, J. R. Brisson, C. P. Ewing, T. J. Trust, P. Guerry, *J. Biol. Chem.* **2001**, *276*, 34862 – 34870.
[5] D. J. McNally, J. P. Hui, A. J. Aubry, K. K. Mui, P. Guerry, J. R. Brisson, S. M. Logan, E. C. Soo, *J. Biol. Chem.* **2006**, *281*, 18489 – 18498.
[6] I. C. Schoenhofen, D. J. McNally, E. Vinogradov, D. Whitfield, N. M. Young, S. Dick, W. W. Wakarchuk, J. R. Brisson, S. M. Logan, *J. Biol. Chem.* **2005**, *281*, 723 – 732.
[7] D. J. McNally, A. J. Aubry, J. P. Hui, N. H. Khieu, D. M. Whitfield, C. P. Ewing, P. Guerry, J. R. Brisson, S. M. Logan, E. C. Soo, *J. Biol. Chem*. **2007**, *282*, 14463 – 14475.
[8] I. C. Schoenhofen, D. J. McNally, J. R. Brisson, S. M. Logan, *Glycobiology* **2006**, *16*, 8C-14C.
[9] D. J. McNally, I. C. Schoenhofen, E. F. Mulrooney, D. M. Whitfield, E. Vinogradov, J. S. Lam, S. M. Logan, J.-R. Brisson, *ChemBioChem*. **2006**, *7*, 1865 – 1868.
[10] a) N. M. Young, J. R. Brisson, J. Kelly, D. C. Watson, L. Tessier, P. H. Lanthier, H. C. Jarrell, N. Cadotte, F. S. Michael, E. Aberg, C. M. Szymanski, *J. Biol. Chem.* **2002**, *277*, 42530 – 42539; b) C. M. Szymanski, B. W. Wren, *Nat. Rev. Microbiol.* **2005**, *3*, 225 – 237.
[11] T. Haselhorst, J. C. Wilson, R. J. Thomson, S. McAtamney, J. G. Menting, R. L. Coppel, M. V. Itzstein, *Proteins: Struct. Funct. Bioinf.* **2004**, *56*, 346 – 353.
[12] J. Angulo, B. Langpap, A. Blume, T. Biet, B. Meyer, N. R. Krishna, H. Peters, M. M. Palcic, T. Peters, *J. Am. Chem. Soc.* **2006**, *128*, 13529 – 13538.
[13] a) A. J. Benie, A. Blume, R. S. Schmidt, W. Reutter, S. Hinderlich, T. Peters, *J. Biol. Chem*. **2004**, *279*, 55722 – 55727; b) O. Berteau, C. Sandstrom, J. Bielicki, D. S. Anson, L. Kenne, *J. Am. Chem. Soc.* **2003**, *125*, 15296 – 15297; c) A. Blume, A. J. Benie, F. Stolz, R. R. Schmidt, W. Reutter, S. Hinderlich, T. Peters, *J. Biol. Chem.* **2004**, *279*, 55715 – 55721; d) V. Jayalakshmi, T. Biet, T. Peters, N. R. Krishna, *J. Am. Chem. Soc.* **2004**, *126*, 8610 – 8611; e) F. Corzana, I. Cuesta, A. Bastida, A. Hidalgo, M. Latorre, C. Gonzalez, E. Garcia-Junceda, J. Jimenez-Barbero, J. L. Asensio, *Chem. Eur. J.* **2005**, *11*, 5102 – 5113; f) T. Haselhorst, A. K. Munster-Kuhnel, A. Stolz, M. Oschlies, J. Tiralongo, K. Kitajima, R. Gerardy-Schahn, M. V. Itzstein, *Biochem. Biophys. Res. Commun.* **2005**, *327*, 565 – 570; g) Y. Yuan, X. Wen, D. A. R. Sanders, B. M. Pinto, *Biochemistry* **2005**, *44*, 14080 – 14089; h) A. Blume, J. Angulo, T. Biet, H. Peters, A. J. Benie, M. Palcic, T. Peters, *J. Biol. Chem.* **2006**, *281*, 32728 – 32740; i) T. Haselhorst, H. Blanchard, M. Frank, M. J. Kraschnefski, M. J. Kiefel, A. J. Szyczew, J. C. Dyason, F. Fleming, G. Holloway, B. S. Coulson, M. V. Itzstein, *Glycobiology* **2006**, *17*, 68 – 81; j) T. Haselhorst, M. Oschlies, T. Abu-Izneid, M. J. Kiefel, J. Tiralongo, A. K. Munster-Kuhnel, R. Gerardy-Schahn, M. V. Itzstein, *Glycoconjugate J.* **2006**, *23*, 371 – 375; k) A. C. Lamerz, T. Haselhorst, A. K. Bergfeld, M. V. Itzstein, R. Gerardy-Schahn, *J. Biol. Chem.* **2006**, *281*, 16314 – 16322; l) R. S. Houliston, N. Yuki, T. Hirama, N. H. Khieu, J.-R. Brisson, M. Gilbert, H. C. Jarrell, *Biochemistry* **2007**, *46*, 36 – 44.
[14] M. Mayer, M. Meyer, *Angew. Chem.* **1999**, *111*, 1902 – 1906; *Angew. Chem. Int. Ed.* **1999**, *38*, 1784 – 1788.
[15] a) B. D. Sykes, *Curr. Opin. Biotechnol.* **1993**, *4*, 392 – 396; b) C. B. Post, *Curr. Opin. Struct. Biol.* **2003**, *13*, 581 – 588; c) M. A. Johnson, B. M. Pinto, *Carbohydr. Res.* **2004**, *339*, 907 – 928.
[16] N. Ishiyama, C. Creuzenet, W. L. Miller, M. Demendi, E. M. Anderson, G. Harauz, J. S. Lam, A. M. Berghuis, *J. Biol. Chem.* **2006**, *281*, 24489 – 24495.
[17] S. T. Allard, K. Beis, M. F. Giraud, A. D. Hegeman, J. W. Gross, R. C. Wilmouth, C. Whitfield, M. Graninger, P. Messner, A. G. Allen, D. J. Maskell, J. H. Naismith, *Structure* **2002**, *10*, 81 – 92.
[18] C. Creuzenet, M. J. Schur, J. Li, W. W. Wakarchuk, J. S. Lam, *J. Biol. Chem.* **2000**, *275*, 34873 – 34880.
[19] Y. S. Wang, D. Liu, D. F. Wyss, *Magn. Reson. Chem.* **2004**, *42*, 485 – 489.
[20] a) H. N. B. Moseley, E. V. Curto, N. R. Krishna, *J. Magn. Res.* **1995**, *108*, 243 – 261; b) V. Jayalakshmi, N. R. Krishna, *J. Magn. Res.* **2002**, *155*, 106 – 118; c) V. Jayalakshmi, N. R. Krishna, *J. Magn. Res.* **2004**, *168*, 36 – 45.
[21] S. Kornfeld, R. Kornfeld, E. F. Neufeld, P. J. O'Brien. *Proc. Natl. Acad. Sci. U.S.A.* **1964**, *52*, 371 – 379.
[22] E. R. Vimr, F. A. Troy, *J. Bacteriol.* **1985**, *164*, 854 – 860.
[23] a) S. Hinderlich, R. Stasche, R. Zeitler, W. Reutter, *J. Biol. Chem.* **1997**, *272*, 24313 – 24318; b) W. Blankenfeldt, M. Asuncion, J. S. Lam, J. H. Naismith, *EMBO J.* **2000**, *19*, 6652 – 6663.
[24] G. M. Morris, D. S. Goodsell, R. S. Halliday, R. Huey, W. E. Hart, R. K. Belew, A. J. Olson, *J. Comput. Chem.* **1998**, *19*, 1639 – 1662.

Received: July 18, 2007
Revised: August 20, 2007
Published online on September 24, 2007

  